Journal of Alloys and Compounds 547 (2013) 18–22

Contents lists available at SciVerse ScienceDirect

Journal of Alloys and Compounds

journal homepage: www.elsevier.com/locate/jalcom

Microstructure and properties of fine grained W–15 wt.% Cu composite sintered by microwave from the sol–gel prepared powders

Y. Zhou, Q.X. Sun, R. Liu, X.P. Wang, C.S. Liu, Q.F. Fang *

Key Laboratory of Materials Physics, Institute of Solid State Physics, Chinese Academy of Sciences, Hefei 230031, People's Republic of China

ARTICLE INFO

Article history:
Received 15 April 2012
Received in revised form 19 August 2012
Accepted 24 August 2012
Available online 9 September 2012

Keywords:
W–Cu composite
Microwave sintering
Hardness
Thermal conductivity

ABSTRACT

The W–15 wt.% Cu composite powders were synthesized by a sol–gel method combining with hydrogen reduction. X-ray diffraction patterns show that pure W and Cu phases were obtained at a reduction temperature of 750 °C for 2 h. The particle size of such powder is in the range from 100 to 400 nm and in each particle the W and Cu phases are seemingly mixed homogeneously in the nanometer scale. The powders were microwave sintered for 25 min at different temperatures of 1050, 1150 and 1200 °C, respectively. The results show that W–15 wt.% Cu samples microwave sintered at 1200 °C exhibit a relative density higher than 97% and an average particle size of W as small as 600 nm. The thermal conductivity and the Vickers microhardness of the sintered W–15 wt.% Cu samples are in the range from 140 to 187 W/m K and from 235 to 347 HV, respectively.

1. Introduction

W–Cu alloys have been widely used in practice as thermal sink, high voltage electric contacts, welding electrodes, etc. [1,2]. These significant applications are owing to the high thermal and electrical conductivity of copper combining with the low thermal expansion coefficient (CTE), high melting points and high hardness of tungsten [3]. However, the immiscibility between W and Cu in thermodynamic equilibrium state makes the W–Cu compacts exhibit very poor sinterability [4], especially for high W content [5]. Meanwhile, the huge gap of melting point between W and Cu makes it difficult to sinter high density W–Cu composites. It has been reported that W–Cu compacts can be fabricated by activated sintering processes, for example by addition of Pd, Ni, Co, Fe and Zn [6,7]. However, these additives could significantly deteriorate thermal and electrical properties of the W–Cu composites. In addition, the sinterability can be improved by enhancing the homogeneity and decreasing particle size of the starting powders. Therefore, quite a number of methods have been exploited to synthesize homogeneous W–Cu composite powders with ultra-fine particle size in recent years, such as mechanical alloying (MA) [8,9], mechano-chemical process [10–12], and homogeneous precipitation process [13]. Among these methods, MA is the most useful for fabrication of compounds that are difficult to prepare by conventional processes owing to the large differences in the melting temperature of the components [8]. However, the milled powder is liable to be contaminated by impurities from the milling and grinding medium.

As a popular method for preparing powders of inorganic materials, sol–gel method has many advantages, such as the relatively low reaction temperature, high purity, and composition homogeneity of products. With regard to consolidation method, metallic powders can be well sintered by microwave sintering [14,15], since metallic powders can absorb microwave efficiently and heat themselves by eddy-current loss [16,17]. Therefore, in this study the W–Cu powders were synthesized by the sol–gel process using citric acid (CA) as chelating agents, followed by reduction of the oxide powders. The high quality W–Cu bulk compacts were obtained by microwave sintering method from such powders, and the microstructure, phase composition, density, hardness, and thermal conductivity were investigated.

2. Experimental procedure

The sol was prepared with analytical reagents of ammonium para-tungstate ($(NH_4)_6H_2W_{12}O_{40}{\cdot}5H_2O$, 99.95%), copper nitrate ($Cu(NO_3)_2{\cdot}3H_2O$, 99.5%) as raw materials and with tartaric acid and citric acid (CA) as chelating agents. The amount of the selected chemical precursors was weighted in mass ratio according to the formula of W–15 wt.% Cu. Then the mixed solution was prepared by dissolving the above four kinds of materials in distilled water, and was stirred vigorously at 60 °C until a transparent gel was formed. The brown gel was heated at 120 °C for 12 h firstly and then calcined at 550 °C for 5 h to obtain the multi-component oxides. Reduction of the multi-component oxide powders was carried out at 750 °C for 2 h in a mixture of 50% hydrogen and 50% argon to produce pure W–15 wt.% Cu powders. Such powders were pressed into a stainless steel die with a uniaxial pressure of 600 MPa to form green samples with a dimension of 13 mm in diameter and 3 mm in height.

* Corresponding author. Tel.: +86 551 5591459; fax: +86 551 5591434.
E-mail address: qffang@issp.ac.cn (Q.F. Fang).

0925-8388/$ - see front matter © 2012 Elsevier B.V. All rights reserved.
http://dx.doi.org/10.1016/j.jallcom.2012.08.143

The green samples were put into a cylinder made of ceramic fibers that were heat insulating and transparent to the microwave. In order to obtain a uniform heating over the whole sample, the cylinder was kept rotating at a speed of 5 rpm during the sintering process. The sintering temperature was monitored by a Ray Tek Infrared Pyrometer. The microwave sintering experiments were conducted in a 3 kW, 2.45 GHz microwave furnace (HAMiLab-V3000, Changsha Synotherm Co. Ltd., China) in a reducing atmosphere (5% H_2 and 95% Ar).

The density of the sintered samples was measured by the Archimedes principle. The microstructure characterization of powder and fracture surfaces of sintered samples was conducted by using field emission scanning electron microscopy (SEM, Sirion 200), and high resolution transmission electron microscopy (HRTEM, JEM-2010F, JEOL). The crystalline phases were identified by XRD analysis (Philips Co. Ltd., X'Pert diffractometer with Cu Kα radiation at 40 kV and 50 mA). Thermal diffusivity (α) was measured by using NETZSCH LFA 457 MicroFlash at room temperature. Accordingly, the thermal conductivity (κ) was calculated from the relationship: $\kappa = c\rho\alpha$, where c and ρ are the specific heat capacity and actual density of the sintered W–15 wt.% Cu mixture, respectively. The specific heat capacity C was determined by theoretical rule of mixtures based on the following formula:

$$C = M_{Cu} \cdot C_{Cu} + M_W \cdot C_W \quad (1)$$

where M_{Cu} and M_W are the mass fraction of Cu and W, and C_{Cu} and C_W are the specific heat capacity of W and Cu at room temperature, respectively. Polished samples were subjected to Vickers microhardness testing under a maximum load of 100 g and a dwell time of 10 s at room temperature.

3. Results and discussion

3.1. Synthesis and characterization of pure W–15% Cu powders

Fig. 1 shows the XRD patterns of precursor powders prepared by annealing the dry gels at 550 °C for 5 h. It can be seen that the main components after the annealing are $CuWO_4$ and WO_3, whose diffraction peaks locate too closely to be separated. The corresponding SEM micrographs of the above precursor oxide powders are shown in Fig. 2. It indicates that the oxide particles aggregate seriously (Fig. 2a) with particle size between 200 and 500 nm (Fig. 2b).

In order to get high quality W–15% Cu powders, it is necessary to investigate the effects of the reduction process. Fig. 3 presents the XRD patterns of the powders prepared at different reduction temperatures from 650 to 800 °C for 2 h in the mixture of hydrogen and argon with a flowing rate of 0.3 L/min. It is found that when the reduction temperature is 650 °C, the original $CuWO_4$ and WO_3 phases were partially reduced into Cu_2WO_4, Cu_3WO_6 and WO_2 phases, and only very small amount of pure W phase can be detected. When the reduction temperature increases to 700 °C, the Cu_2WO_4, Cu_3WO_6 and WO_2 phases still exist but the amount of pure W phase increases. However, when the reduction temperature increases to 750 or 800 °C, all oxide phases disappear and only pure W and Cu phases are detected. These results indicate that to obtain pure W/Cu phases the multi-component oxide powders have to be reduced at least at 750 °C if the reduction time is 2 h.

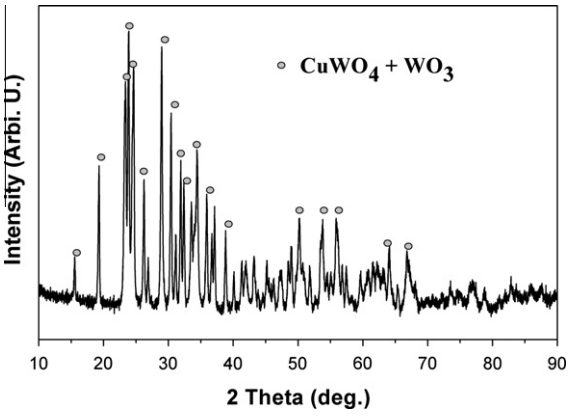

Fig. 1. Powder XRD patterns of dry gels calcined at 550 °C for 5 h.

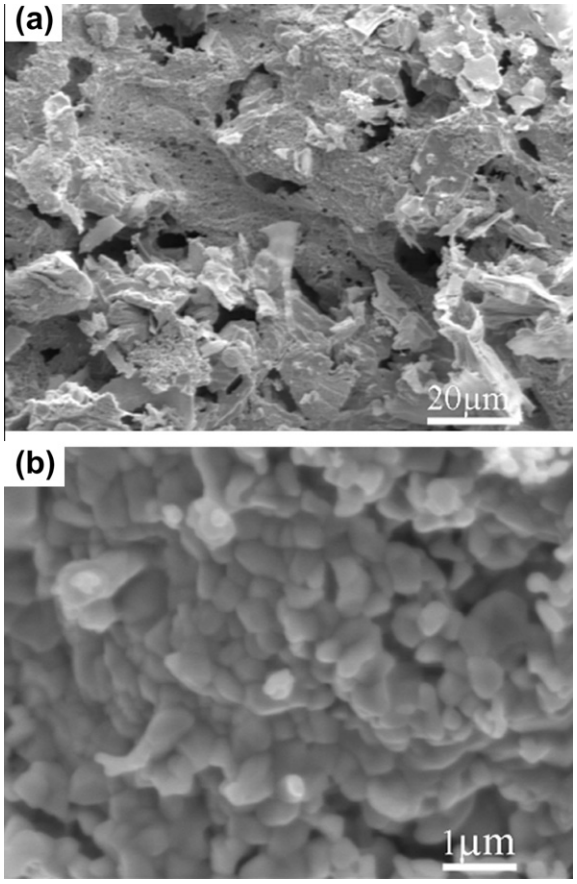

Fig. 2. SEM graphs of dry gels calcined at 550 °C for 5 h: low magnification (a) and high magnification (b).

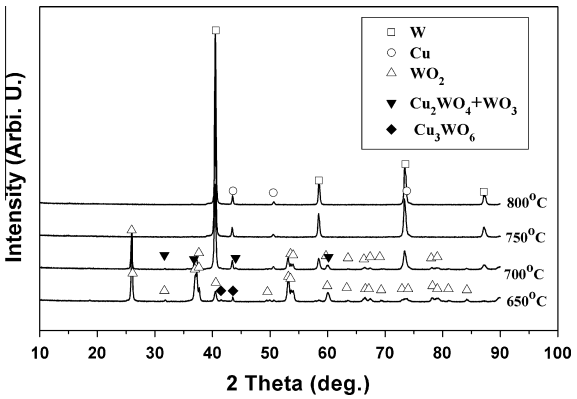

Fig. 3. Powder XRD patterns of W–15% Cu powders at different reduction temperatures from 650 to 800 °C for 2 h in a flowing mixture of hydrogen and argon.

Fig. 4 shows the XRD patterns of the powders reduced at 750 °C for different times of 1, 2 and 3 h. It can be seen that in case of 1 h there are oxide phases of Cu_2WO_4 and WO_2 in the reduced powders. The pure W and Cu phases are obtained for reduction time of 2 and 3 h. So it can be concluded that the reduction temperature of 750 °C and reduction time of 2 h is the optimum condition for preparing pure W–15% Cu powders in the flowing hydrogen and argon.

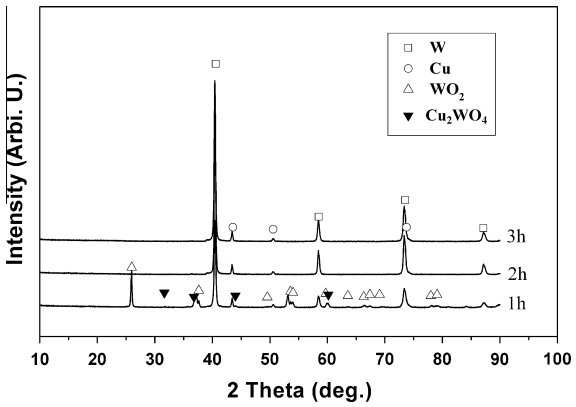

Fig. 4. Powder XRD patterns of W–15% Cu powders reduced at 750 °C for different times in a flowing mixture of hydrogen and argon.

Fig. 5 shows the SEM morphology of W–15% Cu powders reduced at 750 °C for 2 h. It can be seen that after the reduction the particles become as large as 100–400 nm and look like spherical or ellipsoid shape (Fig. 5a). High magnification SEM morphology (Fig. 5b) shows that such particles are not composed of smaller particles like in the un-reduced oxides.

In order to clarify the W/Cu distribution in the W–15% Cu powders, TEM analysis was conducted. In a typical particle as presented in Fig. 6a, elements of W and Cu were detected by EDS (not shown here) in region 1 and 2, where the mass ratio of W and Cu slightly deviates from the designed value, illustrating the uniform dispersion of W/Cu in micrometer scale. To further clarify the phase

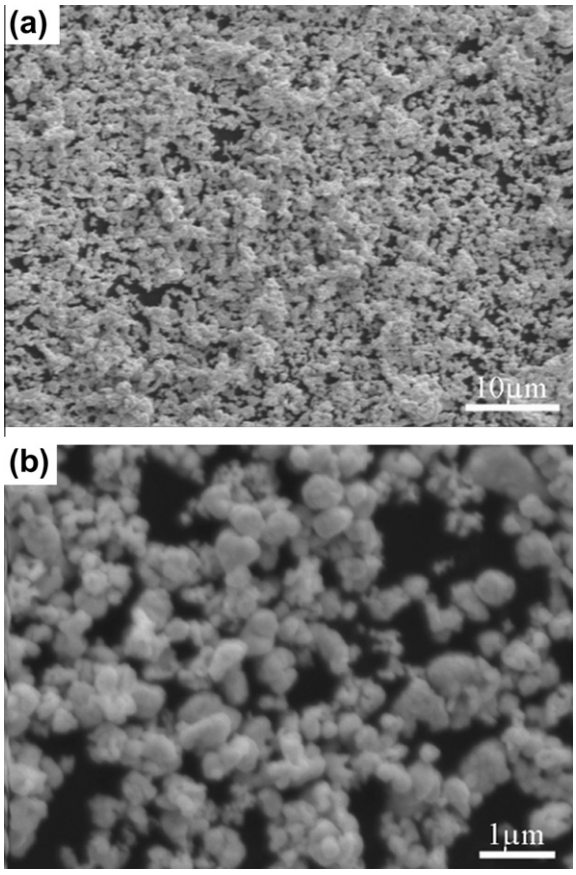

Fig. 5. SEM graphs of W–15% Cu powders reduced at 750 °C for 2 h: low magnification (a) and high magnification (b).

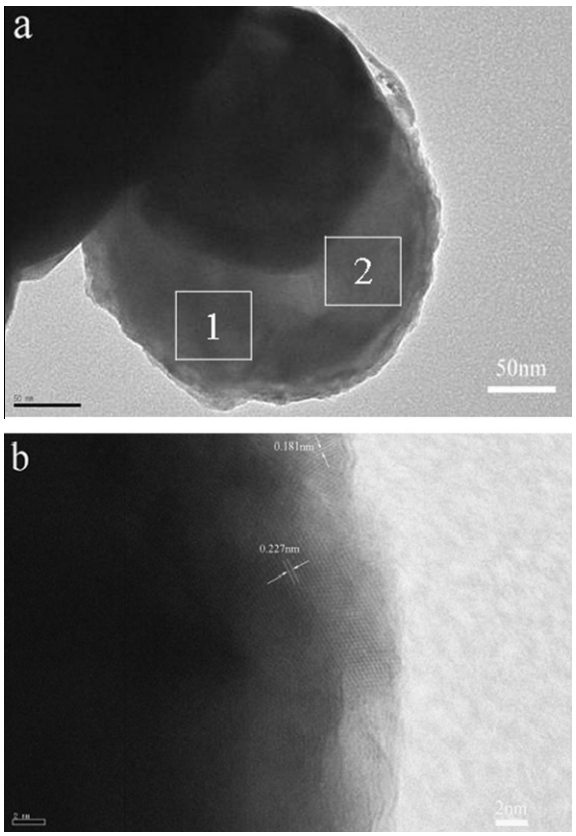

Fig. 6. FETEM photographs of W–15% Cu powders reduced at 750 °C for 2 h: low magnification (a) and high magnification (b).

dispersion of W–15% Cu powder in details, a HRTEM image of this particle was analyzed, as shown in Fig. 6b. It can be seen that in this particle with diameter of about 200 nm, there are many small crystallites with size of several nanometers. Judged from the lattice stripes, these small crystallites are either W or Cu phases. For example, as marked in Fig. 6b, the distance between lattice stripes in one crystallite is about 0.227 nm which is close to the spacing of W (1 1 0) planes (0.2238 nm), while in another crystallite the distance between lattice stripes is about 0.181 nm which is close to the spacing of Cu (2 0 0) planes (0.1808 nm). Therefore, it can be concluded that the W phase and Cu phase is mixed with each other in nanometer scale.

3.2. Microstructure and properties of the sintered samples

Table 1 lists the relative density, Vickers hardness and thermal conductivity of W–15% Cu samples microwave sintered at different temperatures. It can be seen that the properties depend greatly on sintering conditions. As shown in Table 1, the relative density of the sintered samples increases with the sintering temperature. At 1050 °C, a temperature lower than the melting temperature of Cu (1083 °C), the samples only have a relative density of 88.1%. When the samples were sintered at 1150 °C, a relative density of about 93.5% is achieved, and a maximum density of 97.2% is obtained when the samples were sintered at 1200 °C. These results demonstrate that W–15% Cu powders fabricated by reduction of sol–gel process possess good sinterability as long as the sintering temperature exceeds the melting temperature of Cu.

In general, the densification is mainly achieved through solid-phase diffusion when W–15% Cu samples were sintered at temperature below the melting temperature of Cu. Therefore, it is quite difficult to obtain high density samples at 1050 °C because of the immiscibility between W and Cu. This point can be confirmed by

Table 1
Relative density, thermal conductivity and Vickers microhardness of W–15% Cu samples microwave sintered at different temperatures for 25 min.

Sintering temperature (°C)	Relative density (%)	Thermal conductivity (W/m K)	Vickers microhardness (HV)
1050	88.1	140	235 ± 5
1150	93.5	179	325 ± 5
1200	97.2	187	347 ± 5

Fig. 7a, where a few aggregated Cu particles can be observed around the W particles, as identified by the EDS. When W–15% Cu samples were sintered at temperatures above the melting temperature of Cu, the Cu particles became liquid-phase and the dominant sintering mechanism changed into W particle rearrangement [10]. Due to the capillary force and surface tension of Cu-liquid phase, the W particles rearranged promptly and high density W–15% Cu samples can be attained. Fig. 7b and c show the microstructures of W–15% Cu samples sintered at 1150 and 1200 °C. It can be seen that the samples were densely compacted and the net-like Cu phase is homogeneously distributed around the very fine W particles. These results indicate that the fine particle size and the well-dispersed W/Cu in the composite powders are beneficial to the formation of Cu network throughout the whole structure. The W grain size distribution of the above three samples was conducted by counting all grains in the image region from SEM of the fracture surface in Fig. 7a–c and shown in Fig. 7d. At the sintering temperature of 1050, 1150 and 1200 °C, the average grain sizes of W phase are about 300, 400 and 600 nm, respectively. This indicates that increase of sintering temperature will greatly increase the grain size of W phase.

In Table 1 it was also listed the thermal conductivity of W–15% Cu samples, which increases with the sintering temperature. When the consolidated temperature is 1200 °C, the thermal conductivity reaches up to 187 W/m K, which is higher than that of 1150 °C sintered sample (179 W/m K) and 1050 °C sintered sample (140 W/m K). According to the results of relative density and microstructure (Fig. 7) of W–15% Cu samples, the large thermal conductivity in the samples sintered at 1150 and 1200 °C may be owing to the higher density and the formation of Cu network, both of which would result in the higher thermal conductivity. But the thermal conductivity is a little lower than the theoretical value of 223 W/m K for W–15% Cu samples, because there are still about 3% pores in the sintered samples, which may hinder the heat transfer to some extent.

As listed in Table 1, the Vickers microhardness of the sintered samples also increases with the sintering temperature. When the sintering temperatures increase from 1050 to 1200 °C, the Vickers microhardness increase from 235 to 347 HV. The variation of the Vickers microhardness with the sintering temperature can be understood in terms of the relative density.

4. Conclusions

In the present study, W–15% Cu composite powders were synthesized by a sol–gel process using citric acid (CA) as chelating agents, combining with the reduction of the oxide powders. It was found that the reduction temperature of 750 °C and reduction time of 2 h is the optimum condition for preparing pure W and Cu phases in the flowing hydrogen and argon. The particle size of such powders is in the range from 100 to 400 nm and in each particle the W and Cu phases were seemingly mixed homogeneously in the nanometer scale. Such composite powders exhibit good sinterability if the sintering temperature exceeds the melting temperature of Cu. After microwave sintering at 1200 °C for 25 min, the W–15% Cu composite samples exhibit a relative density of about 97%, Vickers microhardness of 347 HV and thermal conductivity as high as 187 W/m K.

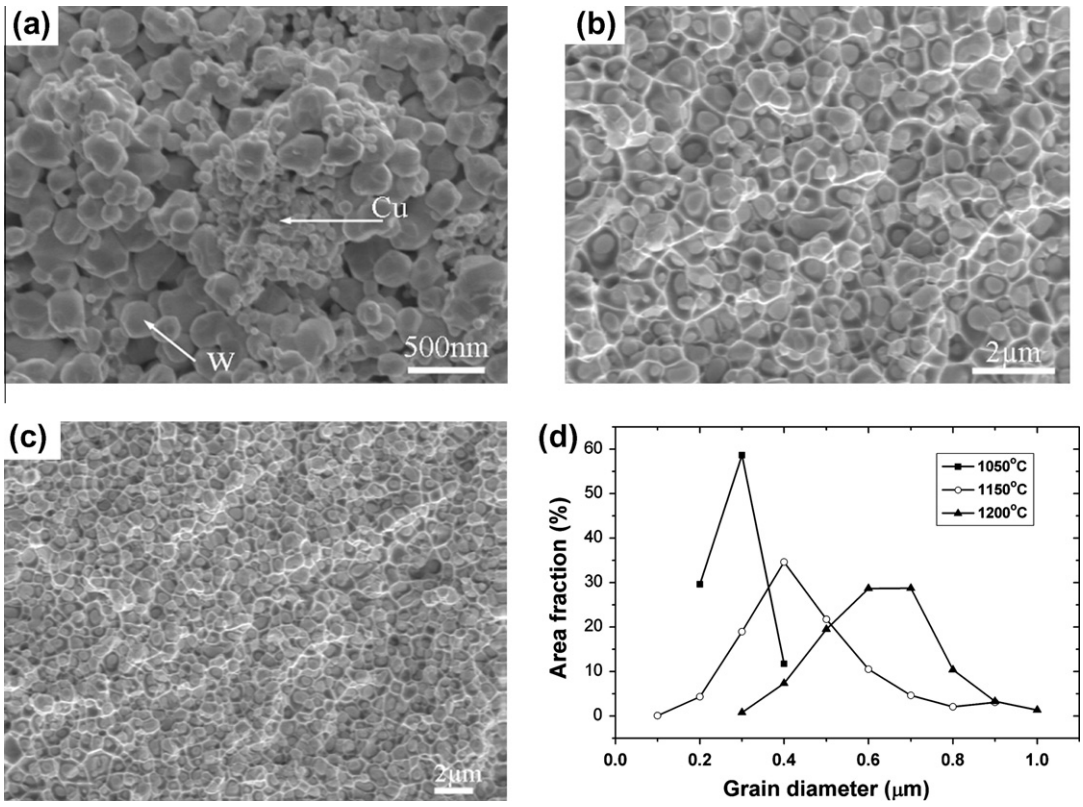

Fig. 7. SEM micrographs of fractured-surface of the samples sintered for 25 min. (a) 1050 °C, (b) 1150 °C, and (c) 1200 °C. (d) The distribution of W grain size in these samples.

Acknowledgments

This work was financially supported by the Innovation Program (Grant No. KJCX2-YW-N35) and Strategic Priority Research Program (Grant No. XDA03010303) of Chinese Academy of Sciences, by the National Magnetic Confinement Fusion Program (Grant No. 2009GB106005), and by the National Natural Science Foundation of China (Grant Nos. 11075177, 91026002, 91126002, 11175203, and 51101152).

References

[1] R.M. German, K.E. Hens, J.L. Johnson, Int. J. Powder Metall. 30 (1994) 205–215.
[2] J.W. David, V.R. Barabash, A. Makhankov, L. Plöchl, T. Slattery, J. Nucl. Mater. 258–263 (1998) 308–312.
[3] S.H. Hong, B.K. Kim, Mater. Lett. 57 (2003) 2761–2766.
[4] T.B. Massalski, Binary Phase Diagram, second ed., ASM, Metal Parks, OH, 1990. p. 1503.
[5] S.S. Ryu, Y.D. Kim, I.H. Moon, J. Alloys Comp. 335 (2002) 233–240.
[6] J.L. Johnson, R.M. German, Int. J. Powder Metall. 30 (1994) 91–102.
[7] P. Chen, G. Luo, M. Li, Q. Shen, L. Zhang, Mater. Des. 39 (2012) 81–86.
[8] S.N. Alam, Mater. Sci. Eng. A 433 (2006) 161–168.
[9] M.H. Maneshian, A. Simchi, Z.R. Hesabi, Mater. Sci. Eng. A 445–446 (2007) 86–93.
[10] D.G. Kim, B.H. Lee, S.T. Oh, Y.D. Kim, S.G. Kang, Mater. Sci. Eng. A 395 (2005) 333–337.
[11] H. Abbaszadeh, A. Masoudi, H. Safabinesh, M. Takestani, Int. J. Refract. Met. Hard Mater. 30 (2012) 145–151.
[12] J.G. Cheng, P. Song, Y.F. Gong, Y.B. Cai, Y.H. Xia, Mater. Sci. Eng. A 488 (2008) 453–457.
[13] J.G. Cheng, C.P. Lei, E.T. Xiong, Y. Jiang, Y.H. Xia, J. Alloys Comp. 421 (2006) 146–150.
[14] R.M. Anklekar, K. Bauer, D.K. Agrawal, R. Roy, Powder Metall. 48 (2005) 39–46.
[15] A. Upadhyaya, S.K. Tiwari, P. Mishra, Scr. Mater. 56 (2007) 5–8.
[16] R. Roy, D. Agrawal, J.P. Cheng, Nature 399 (1999) 668–670.
[17] J. Perelaer, B.J. de Gans, U.S. Schubert, Adv. Mater. 18 (2006) 2101–2104.